EPFL

Theoretical Microfluidics

MICRO-718

T. Lehnert and M.A.M. Gijs (EPFL-LMIS2)

EPFL - Lausanne
Doctoral Program in Microsystems and
Microelectronics (EDMI)







5. Capillary effects and microdroplets

- 5.1 Surface tension and contact angle
- 5.2 The Bond number and capillary flow
- 5.3 Passively driven microfluidic systems
- 5.4 Passive valving in microfluidic devices
- 5.5 Microdroplet generation and applications

Further reading, e.g.: Jean Berthier "Microdrops and Digital Microfluidics", ISBN 978-0-8155-1544-9

"Microfluidics" -- Thomas Lehnert -- EPFL (Lausanne)

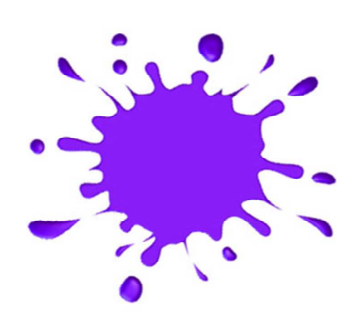
EPFL

5.1 Surface tension and contact angle

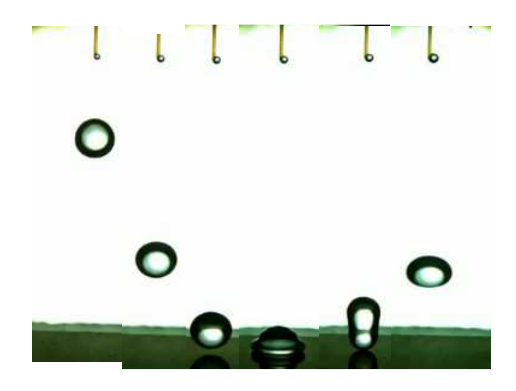
5.1.1 Introduction: Bouncing droplets

- Microsystems have high surface-to-volume ratio $(S/V \sim L^{-1})$.
- Surface forces and interface effects dominate in microfluidics. (rough scale $d \le 100 \, \mu m$, "capillus" (lat.) = "hair")
 - ⇒ Our intuition (based on macroscopic effects) may fail!

Macroscopic effect



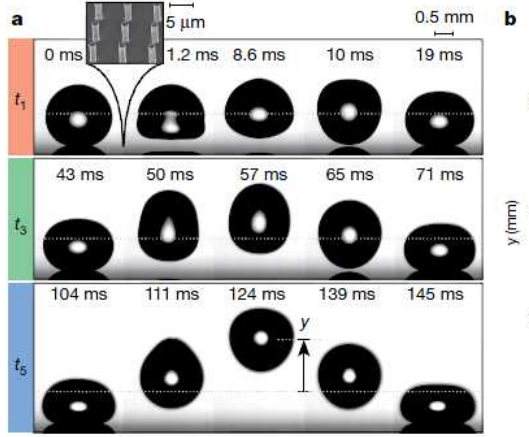


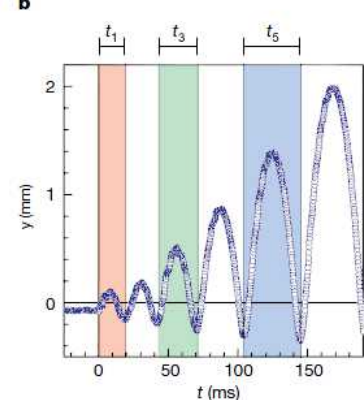


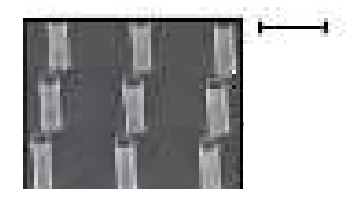
Bouncing water droplet falling onto superhydrophobic surface http://www.youtube.com/watch?v=riXp_Q-fDv8



Spontaneous droplet trampolining on rigid superhydrophobic surfaces.







Silicon superhydrophobic surface with micro-pillars (scale bar 5 µm).

T. Schutzius et al. | Nature | Vol 527 | 82-85 | 2015

Droplet trampolining on a rigid surface. a) High-speed image sequence showing a droplet, initially at rest, trampolining once the environmental pressure is reduced to approximately 0.01 bar (initial droplet radius $R_0 = 0.9$ mm). b) Droplet vertical position y as a function of time t for the image sequence in a. The dotted lines in a correspond to y = 0.

Videos available in supplementary info on the article web-site.

"Microfluidics" -- Thomas Lehnert -- EPFL (Lausanne)



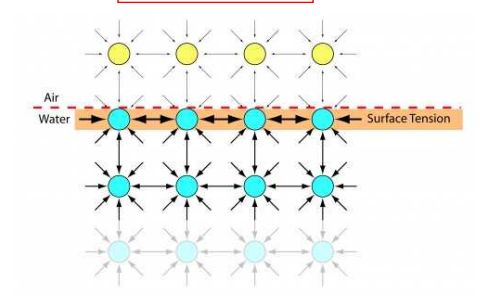
5.1.2 Surface tension

- "Surface tension γ " is the energy required to form an interface between two materials/phases.
- γ is defined as (with Gibbs free energy G of the whole 2-phase system, interface area A):

$$\gamma \equiv \left(\frac{\partial \mathcal{G}}{\partial \mathcal{A}}\right)_{p,T}$$

for
$$T$$
, $p = \text{const}$ $[\gamma]$

for
$$T$$
, $p = \text{const}$ $[\gamma] = \text{J m}^{-2} = \text{N m}^{-1} = \text{Pa m}$ (7.2)



Surface tension for a liquid/gas interface

A molecule in the bulk forms non-permanent chemical bonds, missing bonds at the surface result in **higher energy** than in bulk.

Or: Force imbalance at the interface, forces are redistributed to maintain a force balance (surface tension). Surface liquid molecules experience a net cohesive force towards the bulk.

γ can also be interpreted as "force per length"

$$\frac{F}{w} = \frac{1}{w} \frac{\Delta \mathcal{G}}{\Delta L} = \frac{1}{w} \frac{\gamma \, w \Delta L}{\Delta L} = \gamma. \qquad \text{[N/m]} = \text{[J/m^2]} \tag{7.5}$$

Force required to increase the area $w\Delta L$ of a rectangular surface patch (width w, length L).



• Estimation of γ for a liquid/gas interface assuming one missing bond at the surface. γ increases as the intermolecular attraction increases and molecule size decreases.

$$\gamma \approx \frac{2k_{\rm B}T}{A} = \frac{50~{
m meV}}{(0.3~{
m nm})^2} = 90~{
m mJ~m^{-2}}$$

liquid	$\gamma [{ m mJ/m^2}]$	-
water	72.9	_
mercury	486.5	(table 7.1)
$_{ m benzene}$	28.9	
methanol	22.5	
blood	\sim 60.0	

Experimental values for γ at liquid-vapor interface at 20 °C

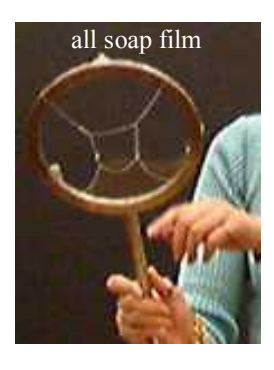
- γ is very sensitive to surface properties and contaminations (and in particular to surfactants), e.g. pure water/air $\approx 70 \text{ mJ/m}^2$, tape water/air $\approx 40 \text{ mJ/m}^2$.
- It is difficult to determine free surface energies of solids (γ_{SL} or γ_{SG}). However, a critical value γ_c can be empirically related to γ_{LG} (Zisman plot: $\cos\theta \sim \gamma_{LG}^{-1}$).
- For $\gamma_{LG} < \gamma_c$ a liquid will fully wet the solid surface, *e.g.* γ_c (copper) ≈ 1100 mJ/m², γ_c (glass) $\approx 250-500$ mJ/m², γ_c (polymer) $\approx 30-50$ mJ/m².
- Surface tension gradients, e.g. $\nabla \gamma(T)$ or $\nabla \gamma(C_{surfactant})$, may induce forces and mass flow along interfaces (Marangoni effect).

"Microfluidics" -- Thomas Lehnert -- EPFL (Lausanne)

EPFL

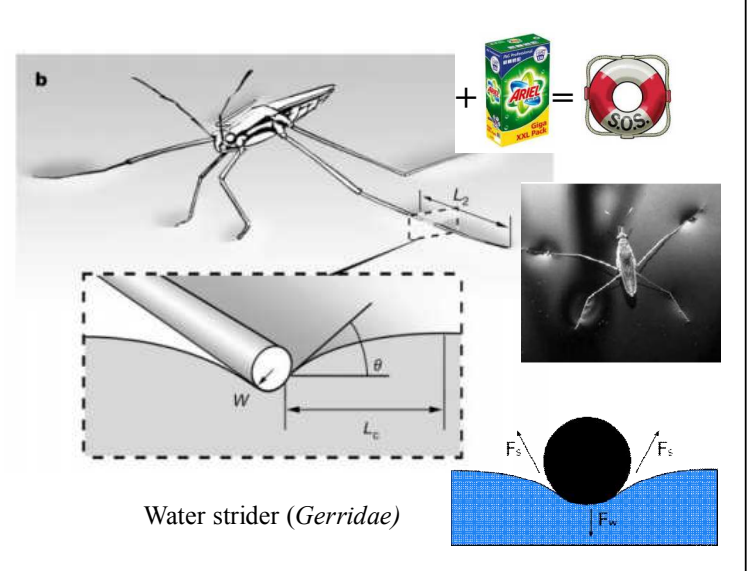
Examples: Surface tension γ acting as force

$$\gamma \equiv \partial G/\partial A$$
 or $\gamma \equiv \partial F/\partial L$





Soap films in a thread mesh, fully covered (left) or partly disrupted (right). Surface tension stretches the thread.



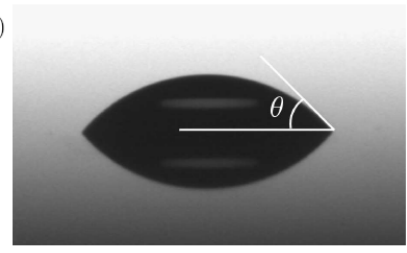
Distortion of the free surface generates a curvature force per unit leg length $F_s = 2\gamma \sin\theta$ that supports the strider's weight F_w .

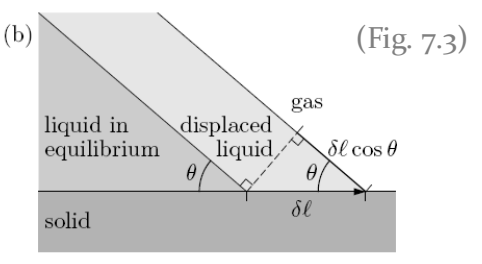


5.1.3 Contact angle and surface wetting

- A contact angle θ appears at the contact line between three phases.
- A contact line forms at solid/liquid/gas or solid/liquid A/liquid B interfaces.
- The contact angle θ is determined by surface tensions $\gamma_{solid/liquid}$, $\gamma_{liquid/gas}$ and $\gamma_{solid/gas}$.







a) Water drop on a plant leaf and on a SiO_2 surface; b) small displacement δl of the contact line

Energy balance at the interface (tilting the liquid/gas interface by an infinitesimal angle $\delta\theta$ results in a shift δl and a change of the Gibbs energy per unit length $\delta G/w$:

$$\frac{1}{w}\delta\mathcal{G} = \gamma_{\rm sl}\delta\ell + \gamma_{\rm lg}\delta\ell\cos\theta - \gamma_{\rm sg}\delta\ell = 0 \tag{7.13}$$

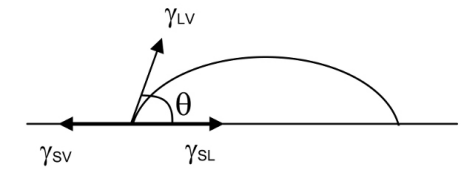
⇒ Young's equation for the contact angle (in equilibrium)

$$\cos \theta = \frac{\gamma_{\rm sg} - \gamma_{\rm sl}}{\gamma_{\rm lg}} \tag{7.14}$$

"Microfluidics" -- Thomas Lehnert -- EPFL (Lausanne)

For solid/water/air interfaces with $0^{\circ} < \theta < 180^{\circ}$ partial wetting occurs. The solid surface is **hydrophilic** if $\theta < 90^{\circ}$ and **hydrophobic** if $\theta > 90^{\circ}$.

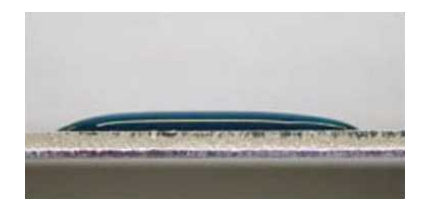
- Complete wetting (spreading of the liquid over the whole surface) occurs for $\theta = 0^{\circ}$, *i.e.* for $\gamma_{SG} \gamma_{SL} > \gamma_{LG}$ (typically for high-energy surfaces like for metals).
- Wetting disappears as the contact angle approches $\theta = 180^{\circ}$, *i.e.* liquids are repelled from surfaces, droplets detach easily (*e.g.* from superhydrophobic surfaces).

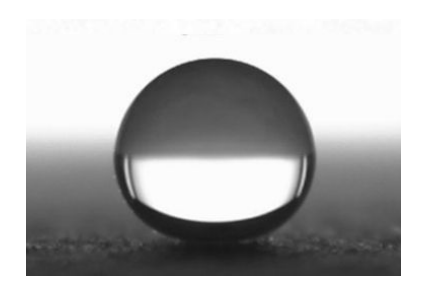


Force representation of the surface tensions at a solid/liquid/vapor contact line (triple point).

 The contact angle depends in a complicated way on the dynamic state of a moving contact line. Due to local defects on the surface, θ is different at the advancing and the receding edge of a moving liquid drop.

EPFL





liquid	solid	θ
water	SiO_2	52.3°
water	$_{ m glass}$	25.0°
water	Au	0.0°
water	Pt	40.0°
water	PMMA	73.7°
mercury	glass	140.0°

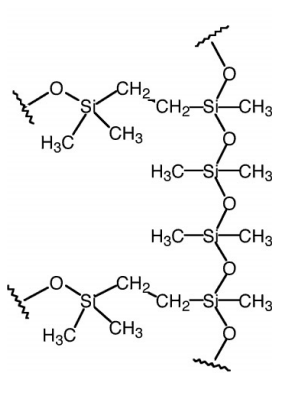
Contact angles in air for different systems (at 20 °C)



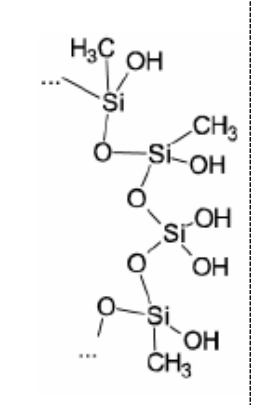
Modification of contact angles by surface plasma treatment

Polydimethylsiloxane (PDMS): PDMS microfluidic devices generally require hydrophilic channels, but native PDMS surfaces are hydrophobic (non-polar CH₃ groups on surface).

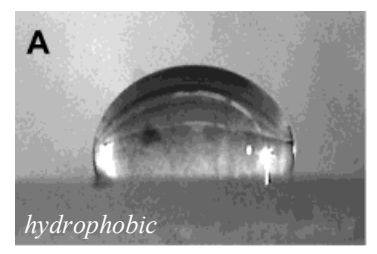
⇒ Surface modification by exposure to air/oyxgen plasma. Formation of polar silanol groups Si-OH on surface generates hydrophilicity.



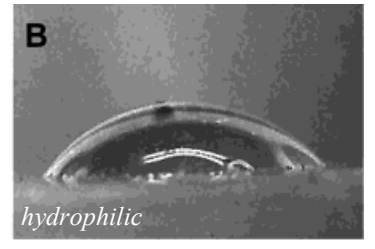
native PDMS surface



PDMS surface after oxygen plasma exposure



Water on an unexposed PDMS surface



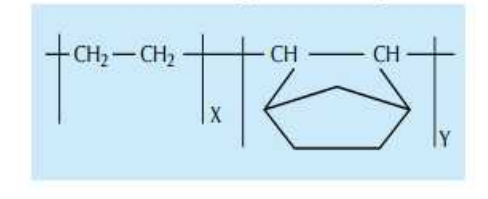
PDMS surface after oxygen plasma for 25s

Brent T. Ginn and Oliver Steinbock, Langmuir 2003, 19, 8117-8118

EPFL

Cyclic Olefin Copolymer (COC, Topas©): The native surface of a COC exhibits a contact angle of 92° with water. For some applications it is essential to have <u>strongly hydrophobic</u> surfaces (*e.g.* on-chip valves).

 \Rightarrow Surface modification by CF_4/O_2 plasma (CH₂/CH surface bonds are replaced by CF).



a)	θ = 21°
b)	θ = 92°
_4	
c)	θ= 136°
	2 1

	[Flow			Power	Duration	Contact
Cas	se Ar	O_2	CF ₄			angle
#	(sccm)	(sccm)	(sccm)	(Watts)	(seconds)	(degree)
1	20	0	0	200	120	~5°
2	10	0	0	150	120	21°
3	10	0	0	100	120	48°
4	10	0	0	25	120	78°
5	0	0	10	100	120	100°
6	0	2	10	150	120	109°
7	0	3	10	150	120	122°
8	0	4	10	200	120	136°

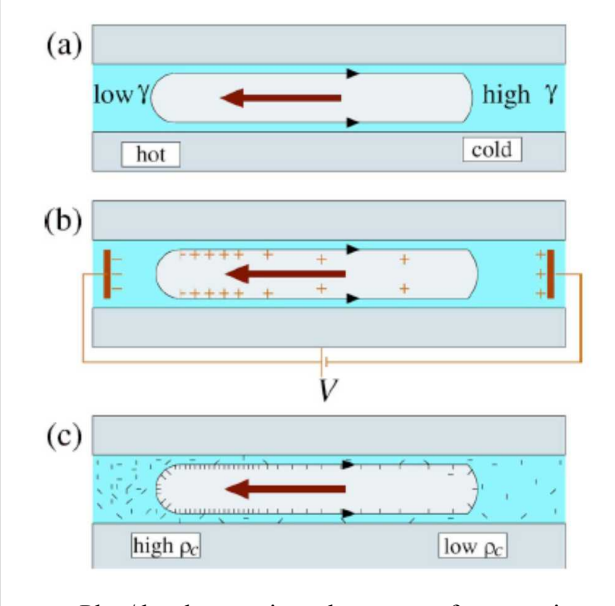
Figure: Modification of the water contact angle on a COC surface by different plasma treatments:

(a) Ar plasma, (b) native COC, (c) CF₄

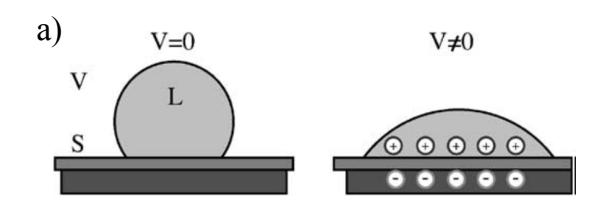
Table: Parameters of various plasma conditions and resulting contact angles.

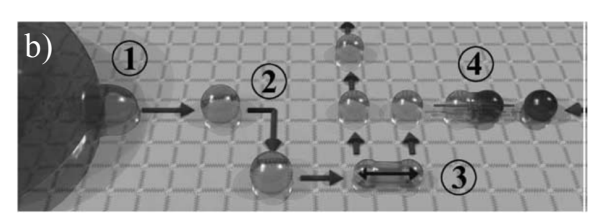
AHN et al., PROC. IEEE, VOL. 92, p. 154-173 (2004)





Plug/droplet motion due to surface tension gradients arising from: a) thermal gradients in the background solution that drive droplets to warmer temperatures; b) electric fields that drive droplets away from the similarly charged electrode; and c) background surfactant gradients that lead droplets to move towards regions of greater surfactant concentration.





(a) Droplet changing its contact angle due to electrowetting. (b) Four main operations of a microfluidic electrowetting array: droplet creation (1), droplet motion (2), droplet splitting (3), and droplet merging (4).

LIENEMANN et al., IEEE Trans. Comput.-Aided Des. Integr. Circuits Syst., 25, 234-2417, 2006

T. M. Squires and S. R. Quake: Microfluidics: Fluid physics at the nanoliter scale, Rev. Mod. Phys., Vol. 77, 977-1026, 2005

EPFL

5.1.4 Young-Laplace pressure

Pressure drop Δp_{surf} occurs across curved interfaces as a consequence of surface tension γ .

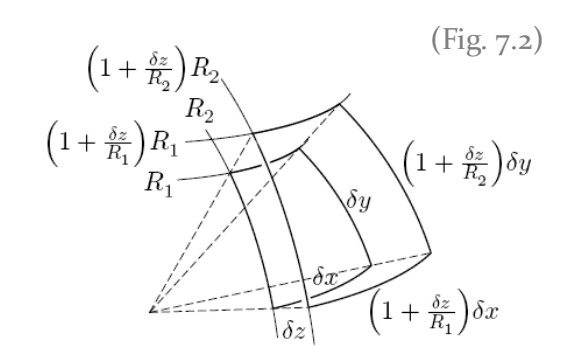
 \rightarrow Evaluation of Δp_{surf} by considering the expansion of a small piece of a curved surface.

Area expansion δA due to a displacement δz

$$\delta \mathcal{A} pprox \left(rac{\delta z}{R_1} + rac{\delta z}{R_2}
ight) \mathcal{A}$$

The surface energy δG_{surf} increases, whereas the pressure-volume energy δG_{pV} decreases upon expansion (equilibrium condition $\delta G = 0$)

$$\delta\mathcal{G} = \delta\mathcal{G}_{\mathrm{surf}} + \delta\mathcal{G}_{\mathrm{pV}} = \gamma \; \delta\mathcal{A} - \left[\mathcal{A} \; \delta z\right] \Delta p_{\mathrm{surf}} = 0$$



⇒ Young-Laplace pressure drop

$$\Delta p_{\rm surf} = \left(\frac{1}{R_1} + \frac{1}{R_2}\right) \gamma \tag{7.8}$$

Sign convention: The pressure is higher in the convex medium, *i.e.* the medium where the centers of the curvature circles are placed.

Example: Water droplet $R = 100 \mu \text{m}$, $\gamma = 70 \text{ mJ/m}^2 \Rightarrow \Delta p_{\text{surf}} = 700 \text{ Pa or 7 mbar}$

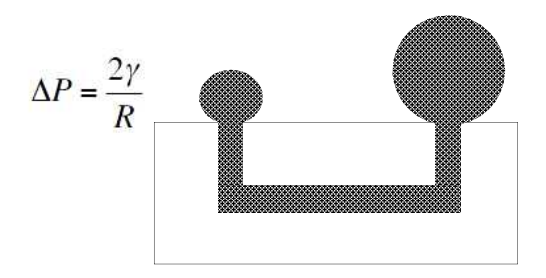
5.1.4 Young-Laplace pressure



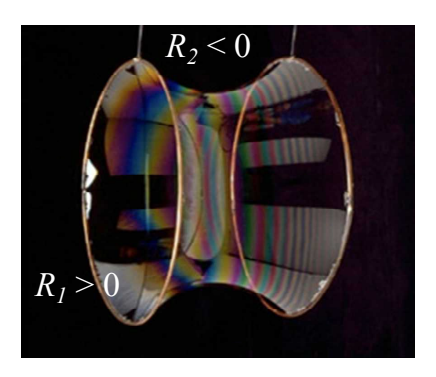


$$\Delta p_{surf} = 4\gamma/R$$

The film of a soap bubble has <u>two</u> interfaces. *p* is higher in smaller bubbles.



Two water droplets of different size connected by a microchannel: *What happens*?



Soap "tube" with open ends: Positive curvature R_1 in azimuthal and negative curvature R_2 in axial direction.

⇒ Young-Laplace pressure drop over interfaces is zero due to open ends

$$\Delta p_{surf} = 0 \qquad \text{thus} \qquad \frac{1}{R_1} + \frac{1}{R_2} = 0$$

⇒ "Mean curvature" of the soap film vanishes

"Microfluidics" -- Thomas Lehnert -- EPFL (Lausanne)

5.2 Bond number and capillary flow

5.2.1 The Bond number

• Energy balance for a volume Ω with a free liquid/air interface taking into account gravity.

$$\mathcal{G}_{\min} = \min_{\Omega} \left\{ \gamma \int_{\partial \Omega} da + \rho g \int_{\Omega} d\mathbf{r} z \right\}$$
 (7.15)

- G_{min} determines the equilibrium shape of the liquid (i.e. spherical for g = 0, deformed for $g \neq 0$).
- Pressure balance for a droplet

$$\frac{\Delta p_{Laplace}}{\Delta p_{hydrostatic}} = \frac{\frac{\gamma}{l}}{\rho g l} \implies \ell_{\text{cap}} \equiv \sqrt{\frac{\gamma}{\rho g}}$$
 (7.16)

- For a water/air interface $l_{\text{cap}} \approx 2.7 \text{ mm}$ at 20°C.
- The capillary length l_{cap} is a characteristic scale. For dimensions $a << l_{cap}$ in a microfluidic system capillary forces dominate over shape deformation related to gravity force.

$$a \ll l_{cap} \rightarrow Bo \equiv \frac{\rho g a^2}{\gamma} = \frac{a^2}{l_{cap}^2} \ll 1$$
 (Bond number)

EPFL







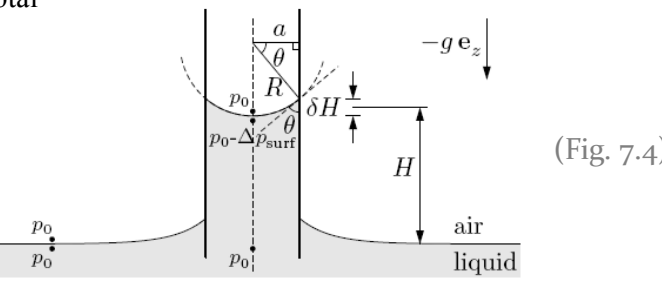
5.2.2 Capillary rise in a vertical circular tube

- If $\gamma_{wet} < \gamma_{dry}$ the system will minimise its total energy by trying to wet the entire surface.

⇒ Capillary filling of hydrophilic tubes

- Interface is spherical for $a << l_{cap}$ (Gravity does not influence the shape)

$$R_1 = R_2 \equiv R = \frac{a}{\cos \theta}$$



$$p_{\mathrm{liq}}(H) = p_0 - \Delta p_{\mathrm{surf}} = p_0 - \frac{2\gamma}{R} = p_0 - \frac{2\gamma}{a} \cos\theta \qquad \tiny{(7.19)}$$

$$p_0 = p_{\text{liq}}(0) = p_{\text{liq}}(H) + \rho g H$$

$$H = \frac{2\gamma}{\rho g a} \cos \theta \tag{7.21}$$



Example: Water in PMMA tube: H = 4.2 cm for a = 100 μ m and H = 42 cm for a = 10 μ m

"Microfluidics" -- Thomas Lehnert -- EPFL (Lausanne)

EPFL

Time dependence of capillary rise

- Considering Poiseuille flow in a circular tube (flow rate Q, meniscus height L(t) and mean velocity V_0)

$$\frac{\mathrm{d}L(t)}{\mathrm{d}t} = V_0 = \frac{Q}{\pi a^2} \approx \frac{a^2 \Delta p(t)}{8\eta} \frac{1}{L(t)} \tag{7.23} \label{eq:7.23}$$

- Viscous pressure drop

$$\Delta p(t) = \Delta p_{\rm surf} - \rho \, g \, L(t)$$

$$- \text{ in } (7.23) \text{ with } \Delta p_{surf} \qquad \qquad \frac{\mathrm{d}L(t)}{\mathrm{d}t} = \frac{\gamma}{8\eta} \left[2a\cos\theta \, \frac{1}{L(t)} - \frac{\rho\,ga^2}{\gamma} \right] = \frac{\rho ga^2}{8\eta} \left[\frac{H}{L(t)} - 1 \right] \qquad \qquad (7.25)$$

- Replacing

$$t = au_{
m cap}\, ilde{t}, \qquad {
m where} \quad au_{
m cap} \equiv rac{8\eta H}{
ho g a^2} \qquad \qquad L = H\, ilde{L}$$

- Results in two approximations

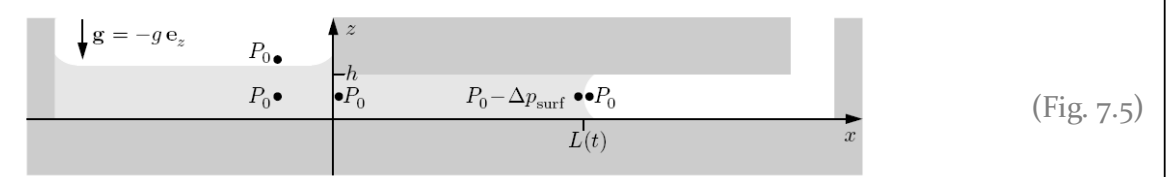
$$\tilde{L}(\tilde{t}) = \sqrt{2\tilde{t}}, \qquad \tilde{t} \ll 1 \qquad \tilde{L} \ll 1$$
 (7.27)

$$\tilde{L}(\tilde{t}) = 1 - \exp(-\tilde{t}), \qquad \tilde{t} \gg 1 \quad \tilde{L} \to 1$$

Example: Water in PMMA tube with $a = 100 \, \mu \text{m}$: $H = 4.2 \, \text{cm}$ is reached in $\tau_{cap} = 3.4 \, \text{s}$

5.2.3 Capillary flow through hydrophilic microchannels



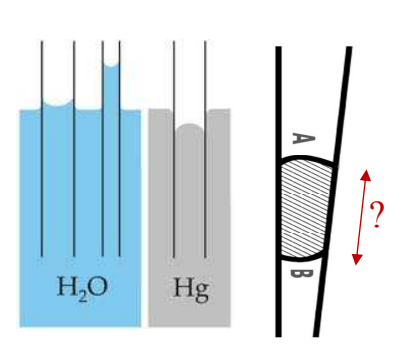


Capillary pump: Young-Laplace pressure drop $-\Delta p_{surf}$ drives liquid through the channel.

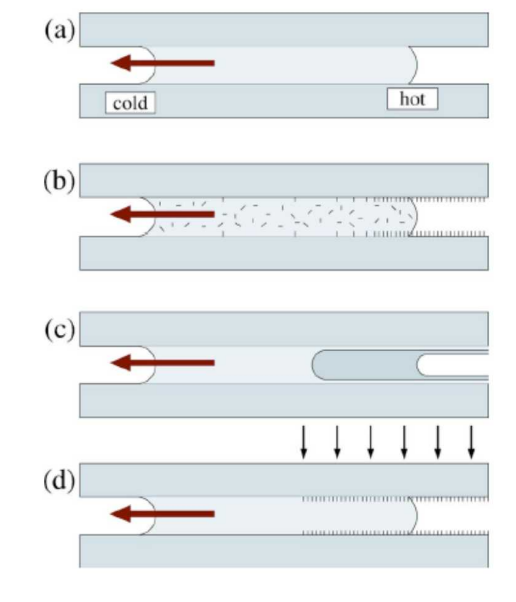
- Poiseuille flow through rectangular channel (h<< w) $Q = h^3 w \Delta p / (12\eta L) \qquad (3.30)$
- Constant Young-Laplace pressure drop at L(t) $\Delta p = \Delta p_{\rm surf} = \frac{2\gamma}{h} \cos \theta \qquad (7.33)$
- Speed of advancing meniscus $\frac{\mathrm{d}L(t)}{\mathrm{d}t} = V_0 = \frac{Q}{wh} \approx \frac{h^2 \Delta p_{\mathrm{surf}}}{12\eta} \frac{1}{L(t)} \tag{7.34}$
 - $L(t) = h \, \sqrt{\frac{t}{\tau_{\rm adv}}} \hspace{0.5cm} \tau_{\rm adv} \equiv \frac{6\eta}{\Delta p_{\rm surf}} = \frac{3\eta h}{\gamma \cos \theta} \hspace{0.5cm} (7.36)$
 - $L(t) = a \, \sqrt{\frac{t}{\tau_{\rm adv}}}, \quad \tau_{\rm adv} \equiv \frac{4\eta}{\Delta p_{\rm surf}} = \frac{2\eta a}{\gamma \cos \theta} \qquad (7.37)$

5.2.4 Tuning of capillary forces and flow





Wetting or non-wetting liquids in a tube (left). Geometrical effect induces liquid plug motion (right).



Plug motion driven by gradients in solid-liquid interfacial energy: a) thermal gradients, b) droplets that contain a chemical that reacts to decrease surface wettability, c) liquid bi-slugs that leave a coating film that lowers the overall surface energy, and d) light-induced reactions that create wettability gradients.

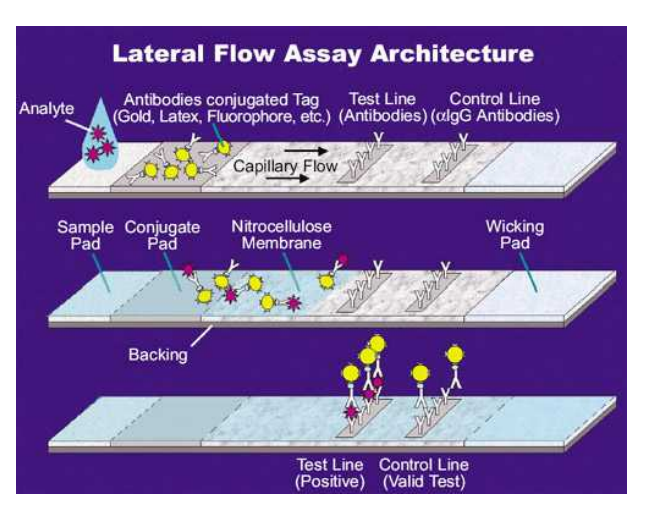
T. M. Squires and S. R. Quake: Microfluidics: Fluid physics at the nanoliter scale, Rev. Mod. Phys., Vol. 77, 977-1026, 2005

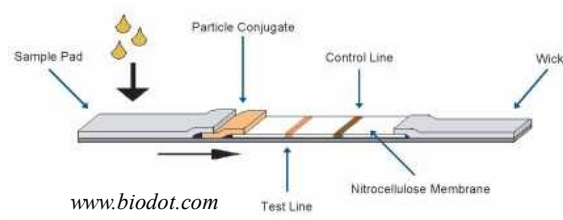
5.3 Passively driven microfluidic systems



5.3.1 Microfluidic chips with integrated capillary pumps

- Rapid point-of-care testing of various analytes with commercial **lateral flow strips** (pregnancy, bacteria, cardiac markers, HIV). Capillary forces drive the sample through a hydrophilic cellulose membrane.
- Results can not be quantitative due to material property variations, *e.g.* effecting the sample flow rate.

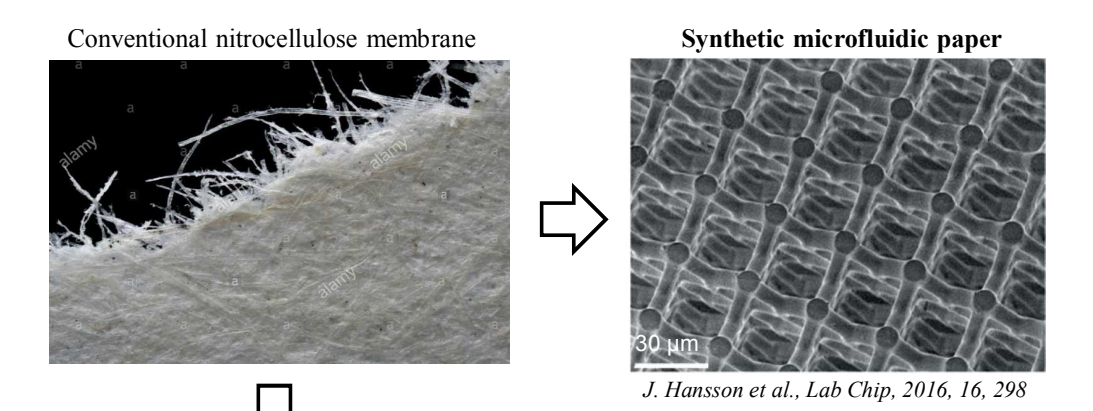




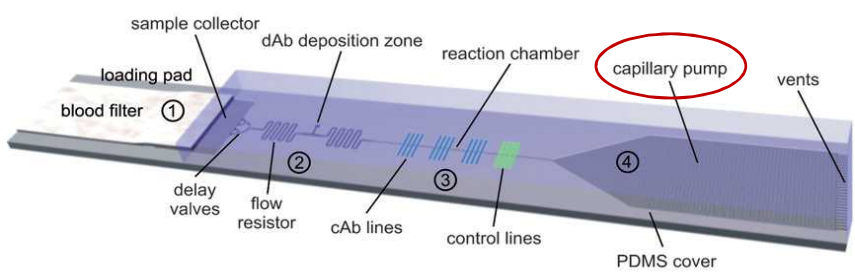
V. Narayanamurthy et al.,
Advances in passively driven
microfluidics and lab-on-chip devices:
a comprehensive literature review and
patent analysis,
RSC Adv., 2020, 10, 11652-11680

EPFL

Options for improving flow control and assay integration



Microfluidic chips inspired by commercial lateral flow strips



L. Gervais et al., Lab Chip, 2009, 9, 3330-3337



Integration of on-chip capillary pumps and circuits

Capillary pumps comprise microstructures of various shapes and size (\sim 10 - 250 μ m) to encode a desired capillary pressure. The pump is preceded by a microchannel, a reaction chamber, capillary retention valve (CRV) and the loading pad.

$$Q = \frac{1}{\eta} \frac{\Delta P}{R_{\rm F}}$$

Q flow rate, ΔP the difference at the front of the liquid, R_F total flow resistance (R_{hyd}/η) , η viscosity.

$$P_{c} = -\gamma \left(\frac{\cos \alpha_{b} + \cos \alpha_{t}}{a} + \frac{\cos \alpha_{l} + \cos \alpha_{r}}{b} \right)$$

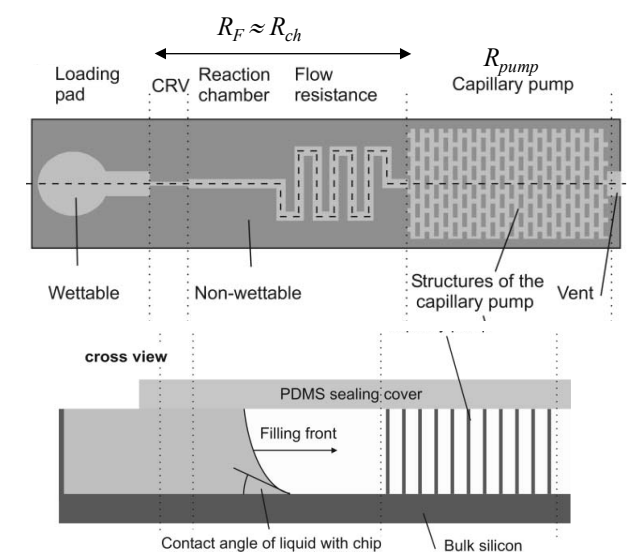
 P_c capillary pressure, $\alpha_{b,l,l,r}$ are the contact angles, a/b channel height/width.

 ΔP and flow resistance R_F define the flow rate (\approx nL/s)

$$R_F \approx R_{ch} >> R_{pump}$$

 $V_{pump} >> V_{channels}$ (here $V_{pump} \approx 0.3 \ \mu L$, area of 15 mm²) Filling time \approx minutes

Review article: A. Olanrewaju et al., Capillary microfluidics in microchannels: from microfluidic networks to capillaric circuits, Lab Chip, 2018,18, 2323



Si chip sealed with PDMS. Contact angles (water): Si (Au coated + thiolated poly(ethylene glycol) 40°, PDMS 115°.

M. Zimmermann et al. Lab Chip, 2007, 7, 119–125

EPFL

Possible capillary pump designs

Simplest design

An extended microchannel having sufficient volume to accommodate all the liquid that needs to be displaced.

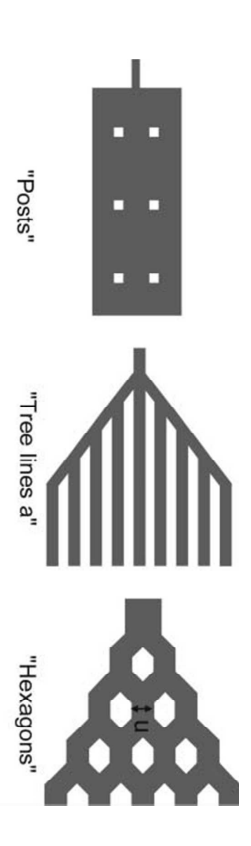
Tree lines

Capillary pressure in the capillary pump can be increased by splitting into smaller parallel microchannels (*but*: total flow resistance can significantly increase for long channels).

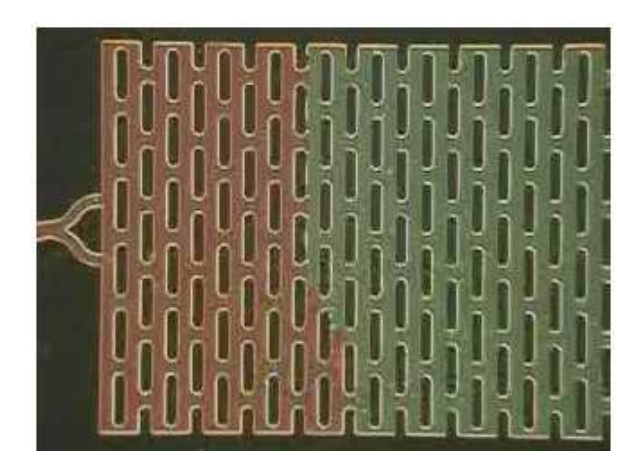
Pump with a regular microstructure array

These capillary pumps have a lower flow resistance because of the large number of parallel flow paths.

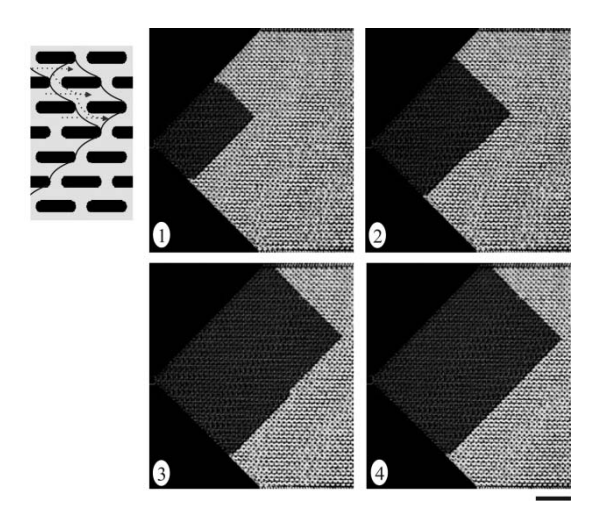
M. Zimmermann et al. Lab Chip, 2007, 7, 119-125



EPFL



Elongated microstructures can be used to control the filling front of a liquid by imposing various time constants for the progression of a liquid along different directions of the capillary pump.



Example of a capillary pump designed to control the shape and orientation of the filling fronts in the capillary pump (scale bar is $500 \mu m$).

Videos in ESI on the article web-site.

M. Zimmermann et al. Lab Chip, 2007, 7, 119–125

"Microfluidics" -- Thomas Lehnert -- EPFL (Lausanne)

5.3.2 Paper-based microfluidic systems

- Paper is now considered an attractive substrate material for microfluidic applications.
- Aqueous liquids are transported through the randomly interwoven cellulose fibres by capillary action.
- Microfluidic paper-based analytical devices ($\mu PADs$) are novel tools capable of analysing complex and small amounts of biochemical samples.

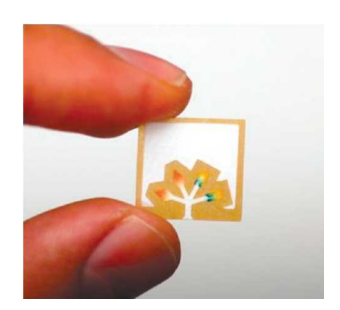
On the right: Chromatography paper patterned with photoresist. The darker lines are cured photoresist, whereas the lighter areas are unexposed paper.

a) Patterned paper after absorbing red ink by capillary action. b) Assay after spotting the reagents. The circular region on the top was used as a control well. c) Negative control using in 5 μ L of artificial urine. d) Positive assay for glucose (left) and protein (right).

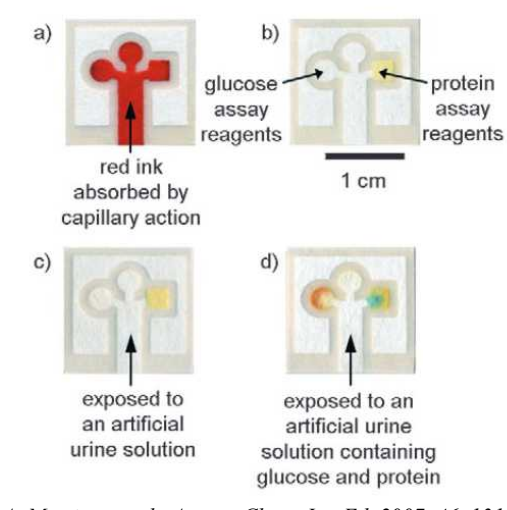
More reviews:

X. Li et al., A perspective on paper-based microfluidics: Current status and future trends, Biomicrofluidics 6, 011301 (2012)

E. Fu et al., Progress in the development and integration of fluid flow control tools in paper microfluidic, Lab Chip, 2017,17, 614-628

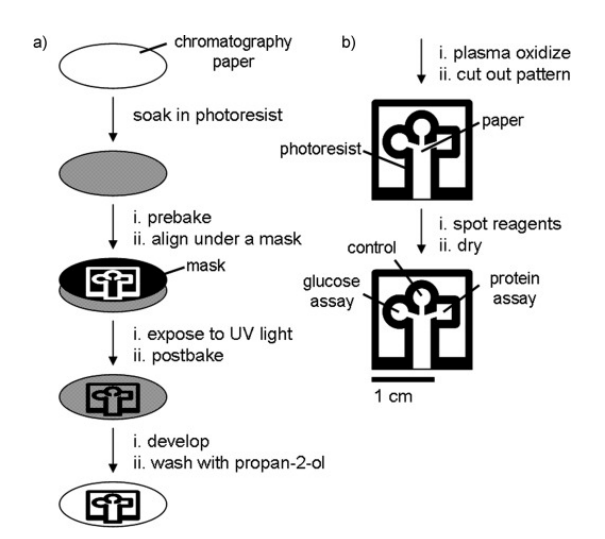


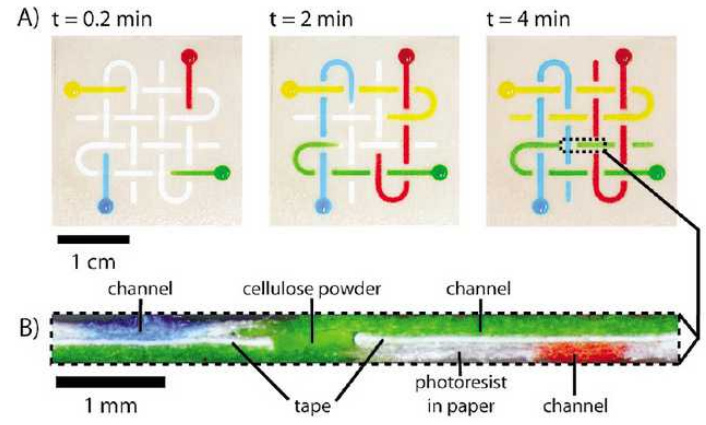
EPFL



A. Martinez et al., Angew. Chem. Int. Ed. 2007, 46, 1318-1320

EPFL





- Diagram depicting the method for patterning a single-layer paper into millimeter-sized channels:
- a) Photolithography was used to pattern SU-8 photoresist embedded into paper; b) the patterned paper was modified for bioassays.
- A. Martinez et al., Angew. Chem. Int. Ed. 2007, 46, 1318–1320
- A. Martinez et al., Anal. Chem. 2010, 82, 3-10

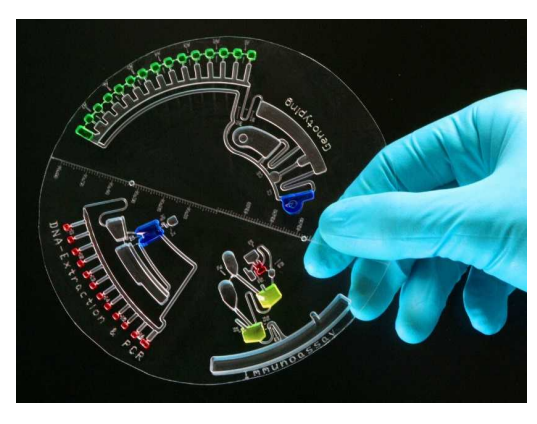
- A) 3D μPAD with four channels that cross each other multiple times in different planes without mixing.
- B) Cross-section of the device in (A). The device is made from two layers of patterned paper and one layer of double-sided adhesive tape. Holes cut through the tape provide contact points between adjacent layers of paper. The holes in the tape are filled with cellulose powder to allow fluids to wick between adjacent layers of paper.

5.4 Passive valving in microfluidic devices



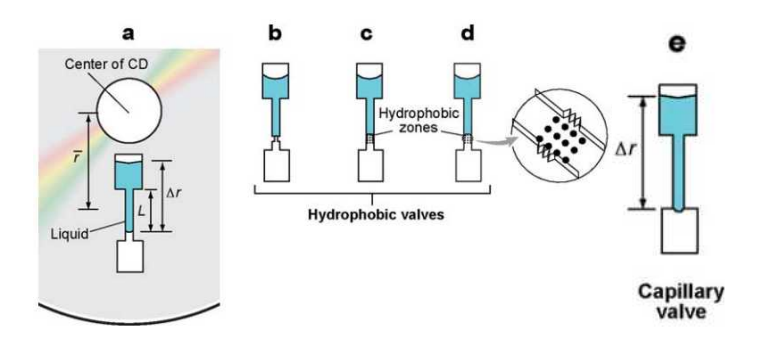
Active microfluidic valves have intrinsic disadvantages limiting the possibilities of on-chip integration (control, high cost, complex structure, difficulty in manufacture).

⇒ Passive microfluidic control (valving) can be achieved by implementing channel portions with specific properties (geometric constrictions, hydrophilic or hydrophobic sections etc.).



Lab-on-a-CD are microfluidic devices that may contain reagents necessary for processing and analysis of (bio-)samples. Fluidic operations are based on centrifugal forces and integrated passive valving.

HSG-IMIT Lab-on-a-Chip Design- & Foundry-Service; www.loac-hsg-imit.de/). © IMTEK.



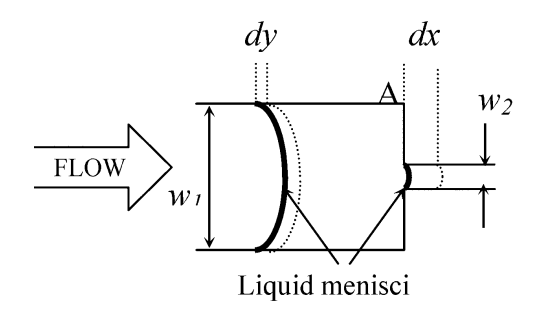
Passive valving for CD microfluidics. (a) Two reservoirs connected by a microfluidic chamber. (b) Hydrophobic valve made by a constriction in a chamber made of hydrophobic material. (c) Hydrophobic valve made by the application of hydrophobic material to a zone in the channel. (d) Hydrophobic channel made by the application of hydrophobic material to a zone in a channel made with structured vertical walls (see inset).

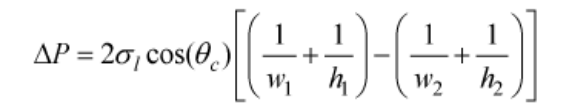
(e) Capillary valve (hydrophilic) made by a sudden expansion in channel diameter, such as when a channel meets a reservoir.

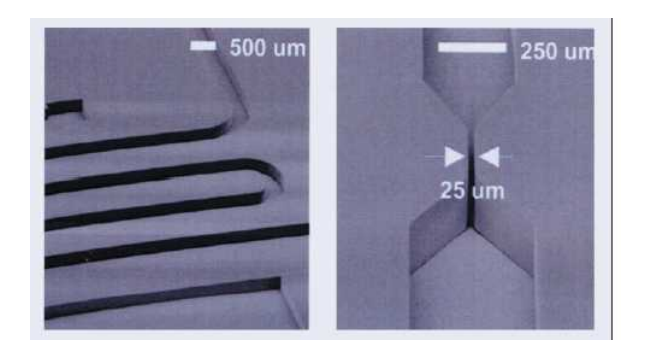
M. Madou et al., Annu. Rev. Biomed. Eng. 2006. 8:601-28



Case study: Constrictions with different geometries in a hydrophobic channel of a pressure-drive device







Microinjected plastic channel and passive valve. The polymer has been plasma-treated to increase hydrophobicity (Cyclic Olefin Copolymer, Topas©).

 ΔP at the channel constriction can be controlled by adjusting the ratio of w_1 and w_2 (generally $h_1 = h_2$).

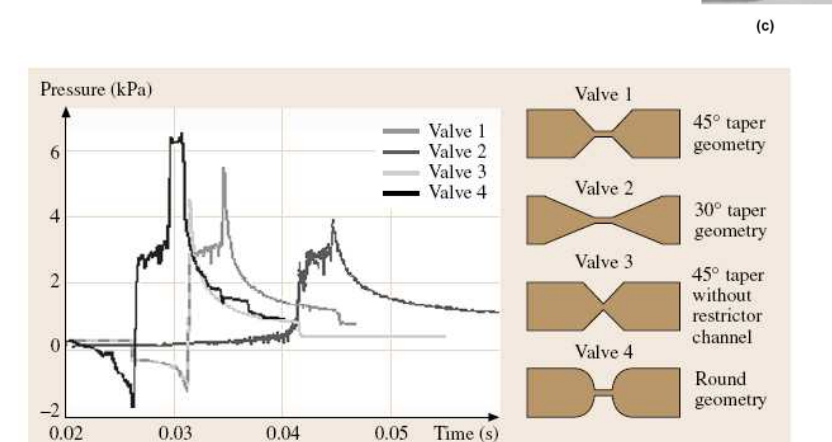
 \Rightarrow Positive pressure drop in <u>hydrophobic</u> channels, *i.e.* a pressure increase is required to push the liquid into the narrow channel.

AHN et al., PROC. IEEE, VOL. 92, p. 154-173 (2004)

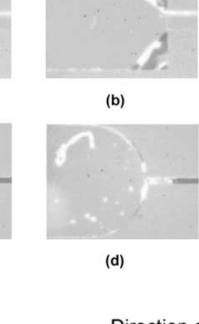
EPFL

AHN et al., PROC. IEEE, VOL. 92, p. 154-173 (2004)

Passive valves have been designed with different geometries to avoid air bubble or fluidic trapping in dead volumes due to abrupt geometrical transitions.

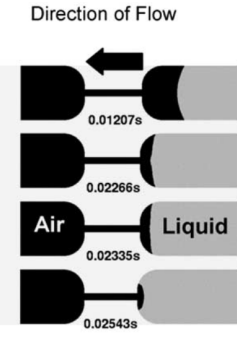


Pressure (monitored at the inlet of the microvalves) required to push the fluid across the different valves with constant flow rate (10 μ L/min).



FLOW.

(a)



Pseudohydrophilic effect: Fluid meniscus gets distorted and changes from convex to concave shape at the valve entrance.

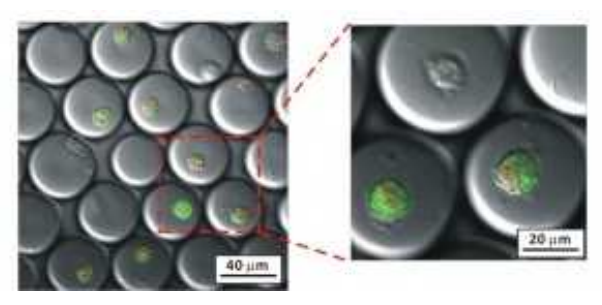
5.5 Microdroplet generation and applications

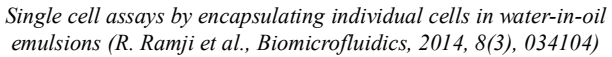


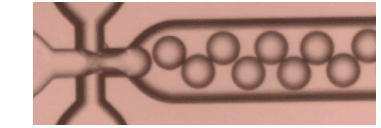
5.5.1 Microdroplets and microfluidics

Emulsions (colloidal suspensions) are multiphase systems of *immiscible* fluids, *e.g.* fat/oil+water in food (milk, butter, mayonnaise), cosmetic creams, paints etc.

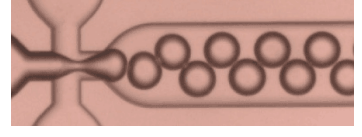
- ➡ Microfluidics: Interfacial/capillary forces become prominent upon downscaling. Surface tension affects the dynamics of the free fluid surfaces and introduces instabilities (even at low *Re* numbers) leading to droplet formation.
- ⇒ Microfluidic systems allow generating monodisperse suspensions with well-controlled droplet size and frequency. The droplet stability in a microchannel depends not only on the fluidic properties but also on interfacial energies/wettability of the fluid/channel boundary.
- ⇒ **Possible applications of droplet microfluidics**: Aqueous nL/pL droplets encapsulated by oil may form confined volumes for chemical microreactors, high-throughput bioassays (encapsulation of cells, protein crystallisation...), nanoparticle fabrication, etc.







100 μm <u>oil droplets in water</u> on a hydrophilic chip



100 µm <u>water droplets in oil</u> on a hydrophobic chip http://www.dolomite-microfluidics.com/

For review see for instance: A. Theberge et al., "Microdroplets in Microfluidics: An Evolving Platform for Discoveries in Chemistry and Biology", Angew. Chem. Int. Ed. 2010, 49, 5846-5868

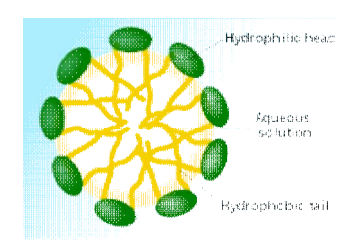
EPFL

Importance of surfactants

Surfactants are amphiphilic molecules that preferentially reside at the interface of two liquid phases (e.g. oil/water). Surfactants have a hydrophilic (anionic, cationic, non-ionic) head and an aliphatic (CH-chain) hydrophobic tail. Surfactants may act as detergents, wetting agents, emulsifiers, foaming agents and dispersants.

Surfactants significantly reduce the interfacial energy thus are required to form small stable droplets. For higher surface tension coalescence is energetically favourable, *i.e.* the emulsion is unstable.

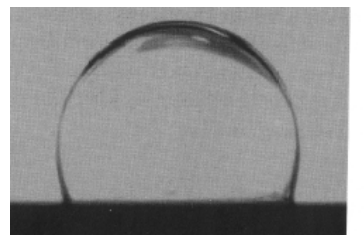
Examples: Phospholipids (lecithin) are food compatible surfactants. Brands for microfluidic applications are Span-80, Tween, Pluronic...

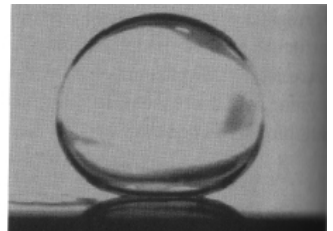


Oil micelle in water: The lipophilic tails of the surfactant ions remain inside the oil because they interact more strongly with oil than with water.

Water droplet in tetradecane (light oil) with lower (on the left) and higher (on the right) surfactant concentration. The water droplet tends to detach from the surface.

(from "Microfluidics", P. Tabeling, Fig. 2.27)







EPFL

5.5.2 Microdroplet generation

- **Monodisperse microdroplet generation in a microfluidic T-junction:** Emulsions are formed by shearing one liquid (water) into a second immiscible fluid (oil). Due to capillary instabilities (surface tension), the flow pattern is not stable as in laminar flow patterns of miscible fluids.
- Competing stress: Viscous shear stress tends to extend and drag the interface, whereas surface tension tends to reduce the interfacial area ⇒ monodisperse pl-sized droplets may form.
- Surfactants (in water or oil) are generally required to stabilize small droplets.

Estimation of the droplet radius R

Shear stress ≈ Interfacial stress (Laplace pressure)

$$\eta(U_0/h) \approx \gamma/R \quad \Rightarrow \quad R \sim \frac{\gamma}{\eta U_0} h = \frac{h}{\text{Ca}}$$

 η viscosity [Pa s]; γ surface tension [N/m] h channel width, U_0 flow speed in main channel (here \approx cm/s!)

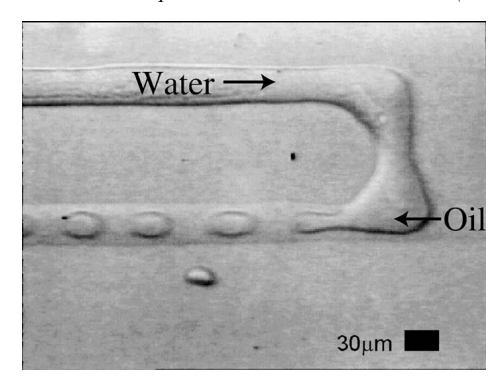
Capillary number (dimensionless)

$$Ca = \eta U_0/\gamma$$

- ⇒ Determines the impact of viscous vs. interfacial effects.
- ⇒ Both are surface forces, no scaling with channel dimension.

For review, see for instance: Han, W., Chen, X. A review on microdroplet generation in microfluidics. J Braz. Soc. Mech. Sci. Eng. 43, 247 (2021).

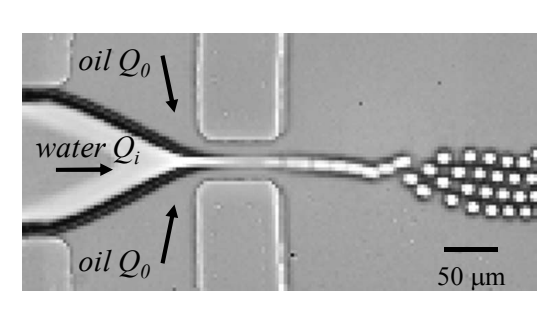
T. Thorsen et al. 86, p. 4163-4166, PHYS REV LETT (2001)



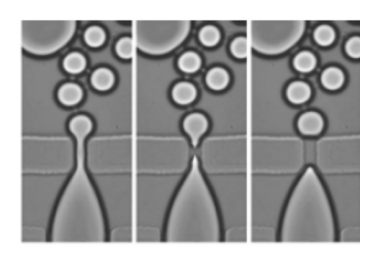
T-junction: Water injected into an oil (+surfactant) stream \Rightarrow Monodispere droplet formation (at 20–80 Hz).

Droplet formation by flow focusing

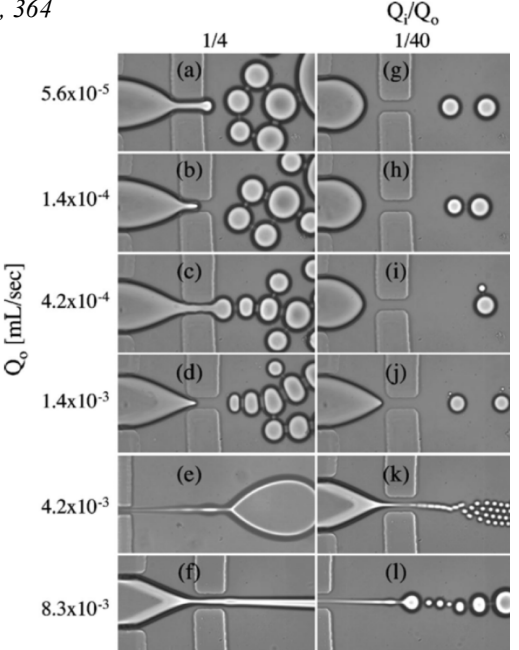
Anna, S. L., N. Bontoux, and H. A. Stone, 2003, Appl. Phys. Lett. 82, 364



Flow focusing of two immiscible fluids. "Rayleigh instability" may lead to the formation of small droplets (water stream Q_i with oil+surfactant sheath flow Q_0 , $\eta=6$ mPas, $Q_0 > Q_i$, PDMS on glass).



Drop breakup inside the orifice



Phase diagram for droplet formation: Depending on Q_0 (for oil) and Q_i/Q_0 different patterns appear such as monodisperse emulsions with droplet sizes equal or smaller to the orifice diameter (\approx 40 μ m), polydisperse suspensions, long threads, satellites, etc.

Formation of droplets of alternating composition

Zheng et al., Anal. Chem. 2004, 76, 4977-4982

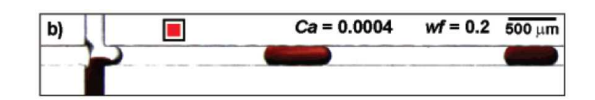
EPFL

a) Schematic of the injection channels. $Ca = \eta U_0/\gamma$



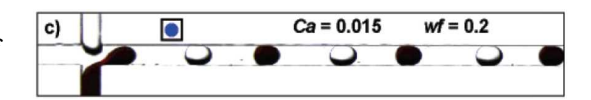
b) Ca < 0.001

Surface tension dominates. The aqueous streams reach the inlet junction head to head and coalesce.



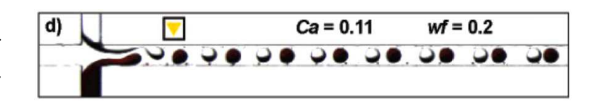
c) 0.001 < Ca < 0.05

The aqueous streams snap off cleanly. A steady array of alternating droplets is generated in the main channel.



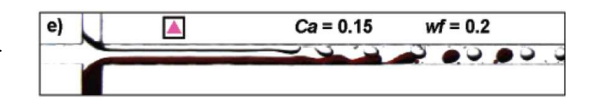
d) 0.05 < Ca < 0.13

Shear forces become larger. Competition between shear force and surface tension. Droplets smaller than the cross-section of the channel form.



e) 0.13 < Ca

Shear forces dominate. Aqueous streams form a laminar segment beyond the junction before droplets can form.

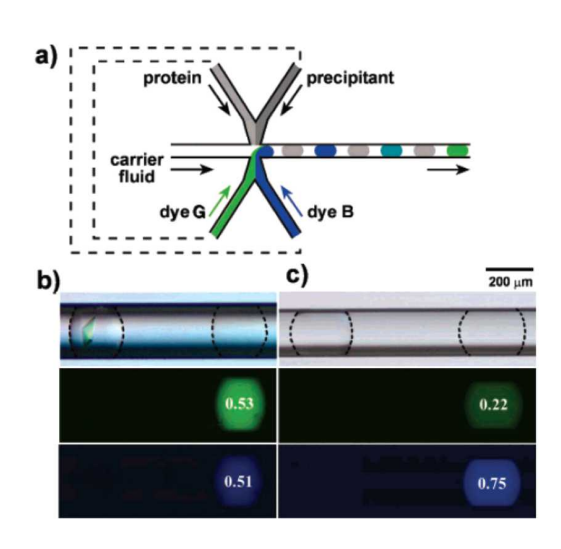


Device parameters: Carrier fluid PFO in PFP (10%, v/v; $\approx 2.0 \,\mu\text{L/min}$, $\eta = 16 \,\text{mPas}$) + two aqueous solutions (glycerol, $\eta = 16 \,\text{mPas}$), water fraction (wf) is defined as the ratio of the water to total flow rates; Geometry: cross-junction, channel width 200 μ m.

EPFL

Application: Indexing of droplet composition during protein crystallization by forming stable alternating sets of "reaction droplets" and "marker droplets". Droplets were formed for conditions that yield/do not yield thaumatin crystals.

- (a) Syringes holding thaumatin and dye G solutions were driven by one syringe pump. Syringes holding the precipitant and dye B solutions were driven by another one.
- (b),(c) top: a polarized light microphotograph showing a droplet (left) containing a mixture thaumatin/precipitant next to a droplet (right) containing a corresponding dye G / dye B mixture.
- (b),(c) middle: Fluorescence from dye G (fluorescein). The intensities (0.53/0.22) indicate the relative concentration of thaumatin.
- (b),(c) bottom: Fluorescence from dye B. The intensities (0.51/0.75) indicate the relative concentration of the precipitant.



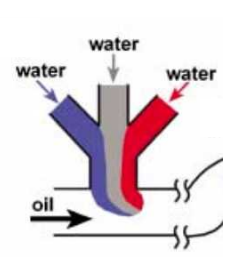
B. Zheng et al., Anal. Chem. 2004, 76, 4977-4982



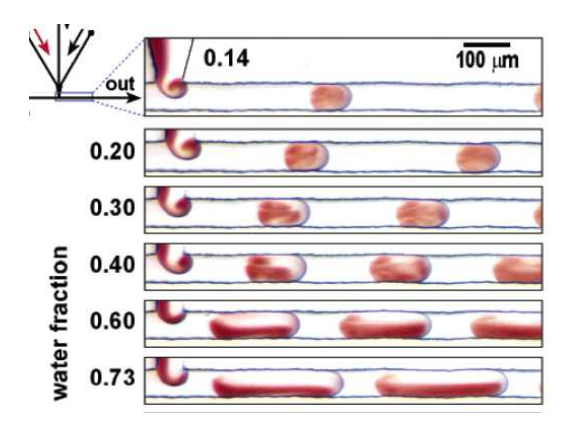
5.5.3 Rapid mixing in droplets by chaotic advection

Aqueous droplets/plugs of multiple solutions of reagents in a continuous flow of a water-immiscible fluid may act as microreactors. Shear forces generate internal flow patterns that mix the reagents. Fluidic transport with no dispersion.

At low *Re* laminar flow is preserved during plug formation. In <u>straight channel segments</u> two steady internal counterrotating flows form with moderate mixing performance. Reagent solutions end up in two halves of the plug. Twirling during injection slightly improves mixing in small plugs.



Plug formation at low *Ca* **numbers** (< **0.1).** Droplets are large enough to block the channel but do not wet the walls. The surface tension at the water/PDMS interface has to be higher than at the water/oil interface.

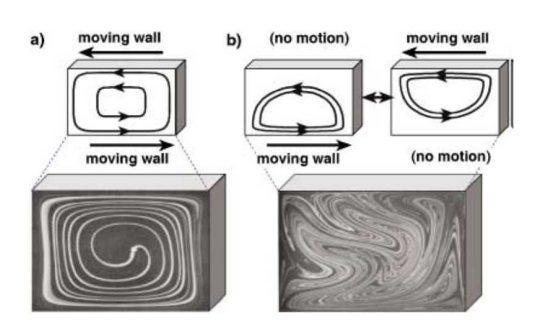


Microphotographs of different length plugs near the plug-forming region as a fct of water fraction. Inlet: aqueous KNO₃ solutions (1 red + 2 colorless) + perfluorodecaline (carrier fluid). Hydrophobic PDMS channel, 50 mm/s, plug size 100 nl-range, laminar flow conditions ($Re \approx 1-10$, $Ca \approx 10^{-3}-10^{-2}$).

J.D. Tice et al., Langmuir 2003, 19, 9127-9133

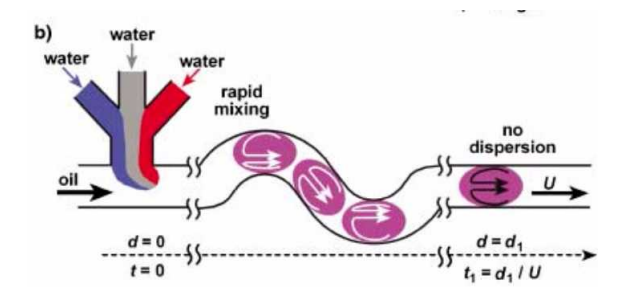


Internal circulating flow patterns in plugs driving down a <u>winding channel</u> experience a baker's transformation \Rightarrow Rapid mixing on the ms-scale.



Flow patterns of mixing by steady (a) and timeperiodic (b) flows in a flow cavity. Horizontal walls move as shown.

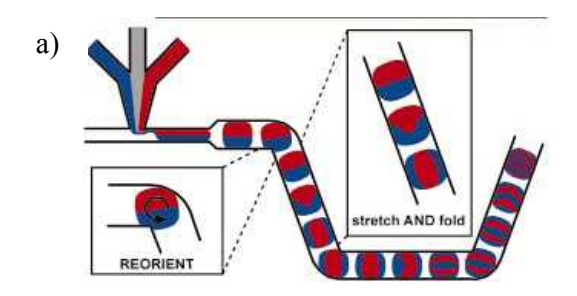
Song, H. et al, Appl. Phys. Lett. 83, 4664 (2003) Song et al., Angew. Chem., 42, 767 (2003)



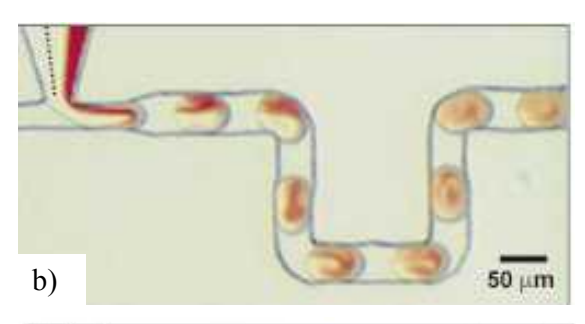
A plug moving through a curved part of a winding channel moves at different velocities relative to the walls. When the channel changes direction, the axis of the circulating flow changes. The internal flow pattern is similar to fluid in a flow cavity with time-periodic flows (see on the left).



Experiments show that the mixing length varies ~log Pe, i.e. mixing is based on chaotic advection.



Mixing by the baker's transformation in plugs moving through winding channels shown (a) schematically and (b) experimentally. (c) A false-color microphotograph of plugs showing time-averaged fluorescence arising from mixing of Fluo-4 and Ca²⁺ solutions (individual plugs are not visible!).





Song, H. et al, Appl. Phys. Lett. 83, 4664 (2003) Song et al., Angew. Chem., 42, 767 (2003)

"Microfluidics" -- Thomas Lehnert -- EPFL (Lausanne)

EPFL

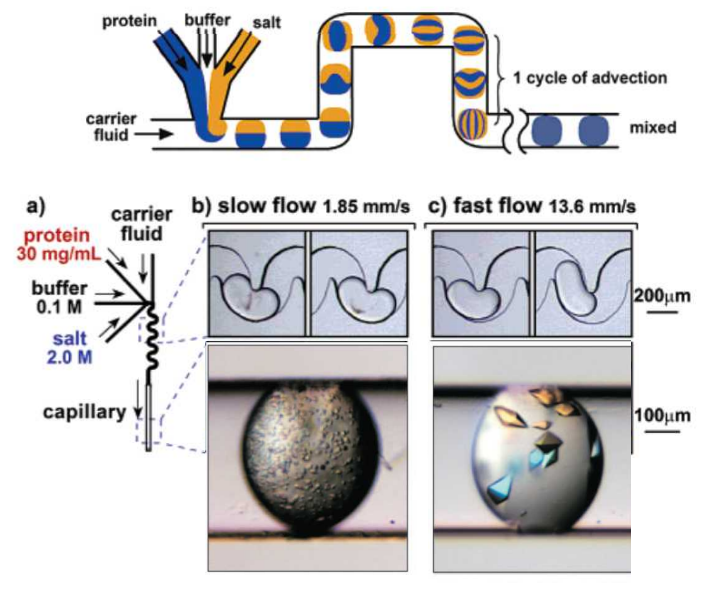
Application 1: Protein crystallization in droplets/plugs

Nucleation is an important aspect of protein crystallization. The number of crystal nucleation events depends the area and the lifetime of the <u>fluidic interfaces</u>. Plug-based microfluidic systems are suitable to tune mixing effects of protein and salt solutions (precipitants).

Fig. a) Plug-based microfluidic setup. The mixing speed may be controlled by varying the total flow rate.

Fig. b) Rapid nucleation at low flow velocity. Precipitation or showers of microcrystals appear after incubation.

Fig. c) At high flow velocity (more rapid mixing and shorter interface lifetime) no precipitation occurred and only a few large crystals grew.



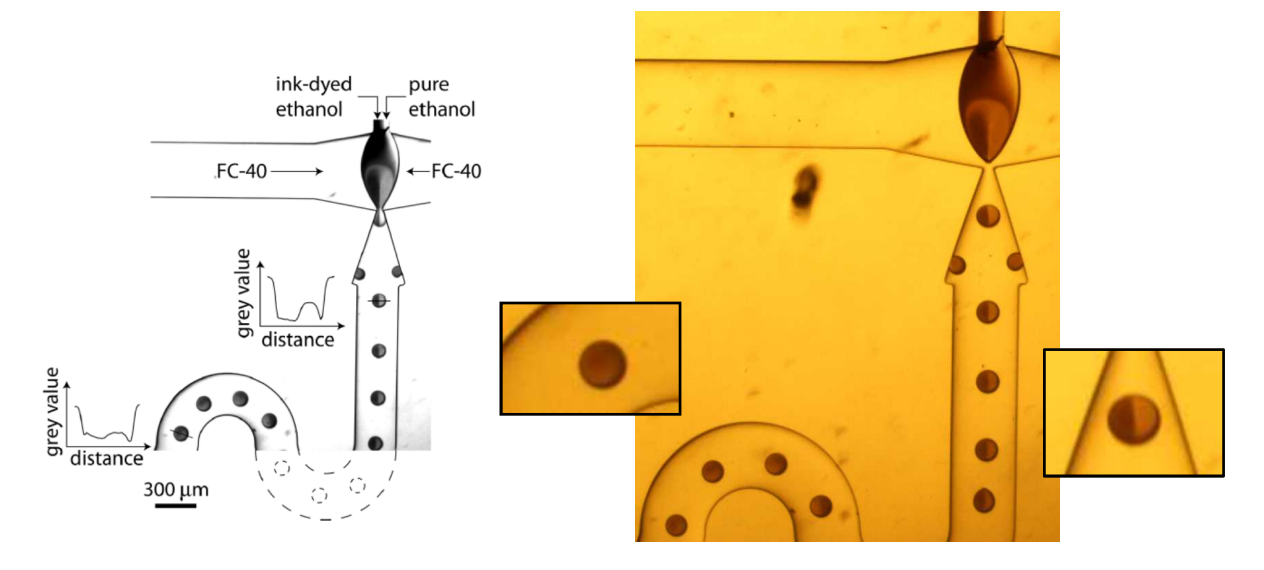
nL-volume aqueous plugs containing protein (thaumatin) and precipitant (2 M $KNaC_4H_4O_6$) solutions; fluorinated carrier fluid. PDMS channels are connected to a glass capillary. Incubation time $8h/18^{\circ}C$.

Zheng et al., Current Opinion in Structural Biology 2005, 15:548–555 Chen et al., J. AM. CHEM. SOC. 2005, 127, 9672-9673



Application 2: Nanoparticle synthesis

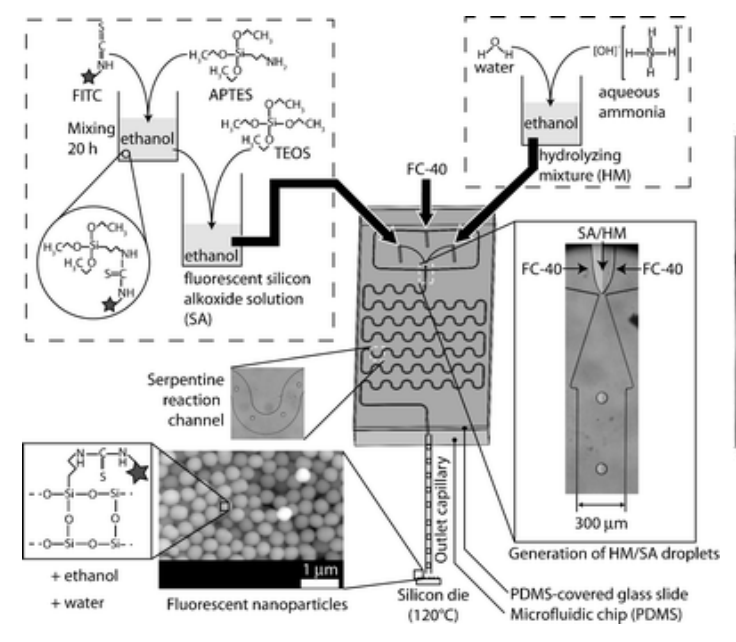
J. Wacker et al., Lab Chip, 2012, 12, 3111-3116

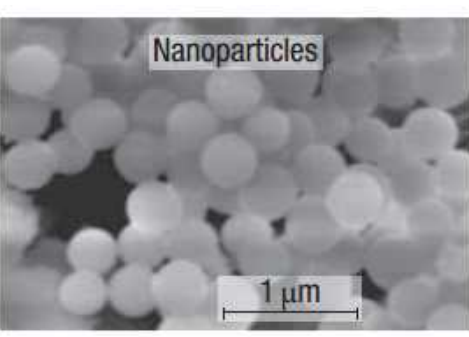


Demonstration of mixing performance: Ink-dyed ethanol and pure ethanol is injected in the center inlet, FC-40 (a fluorocarbon-based oil) from the side channels. After only two U-turns, the intensity profile of a bicolored droplet flattened dramatically, indicating fast mixing (video taken at 1000 frames/s).

"Microfluidics" -- Thomas Lehnert -- EPFL (Lausanne)

EPFL





J. Wacker et al., Lab Chip, 2012, 12, 3111-3116

Droplet-based synthesis of fluorescent SiO_2 nanoparticles: A fluorescent silicon alkoxide (SA) precursor solution and a hydrolysing mixture (HM) are mixed in droplets and collected in an outlet capillary. After evaporation of the reagents, the SiO_2 nanoparticles (\varnothing 50–350 nm) are analysed by electron microscopy.

5.5.4 Single-cell high-throughput screening

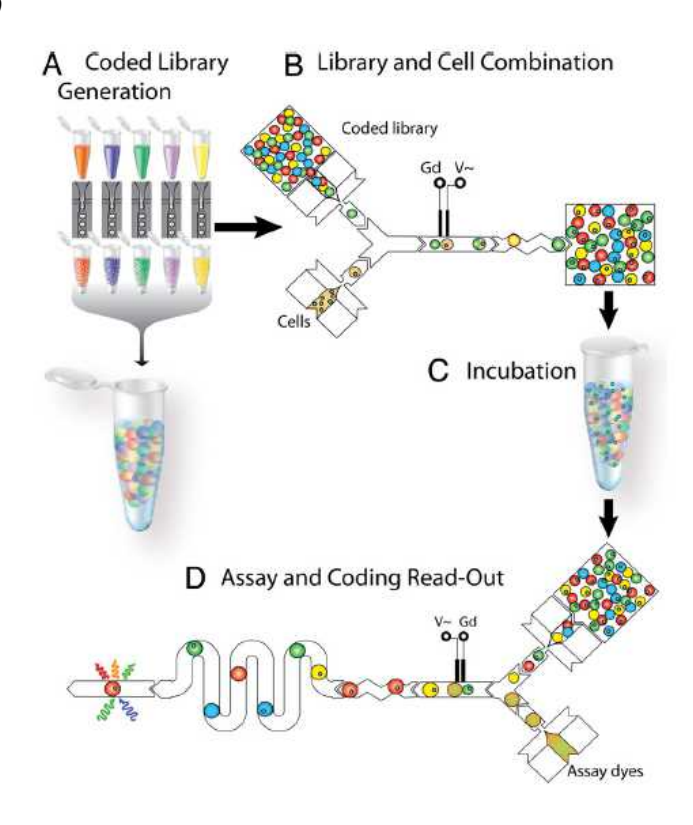


Brouzes E et al. PNAS 2009;106:14195-14200

Application: Screening of a drug library for cytotoxic effects (On-chip cell viability assay).

The 4 steps of the droplet screening work flow:

- (A) The drug library is formatted into a droplet emulsion with each member uniquely coded with an optical label.
- (B) Each library droplet is combined with a cell-containing droplet on a merge chip.
- (C) The emulsion is incubated for cell treatment (off-chip, 24h).
- (D) The emulsion is reinjected into the assay chip. Each droplet's fluorescence is measured for both assay and drug coding readouts.



"Microfluidics" -- Thomas Lehnert -- EPFL (Lausanne)



Cell encapsulation

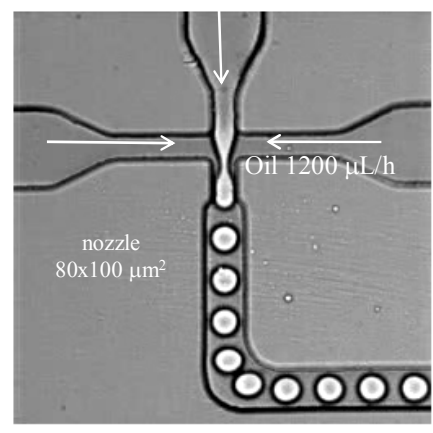
Droplets are generated by infusing the cell suspension into opposing streams of the carrier fluid at a flow-focusing nozzle (700 pL, rate of 100 droplets/s).

Cell encapsulation follows a Poisson distribution that defines the droplet occupancy statistics. About 30% of the droplets contain a single-cell.

Cell type: U937 cells (human white blood cells)

Drug-containing droplets (200 pL) with different concentrations are formed in a similar way in a separate device.

Cell suspension (250 μL/h)



Droplet Generation

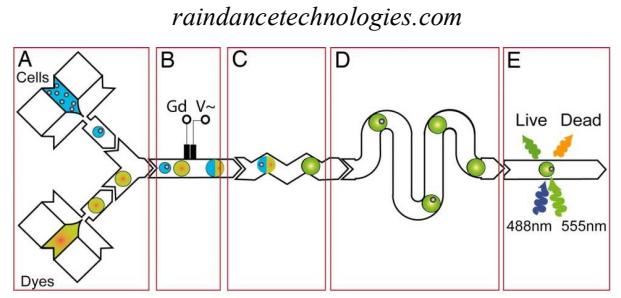
raindancetechnologies.com

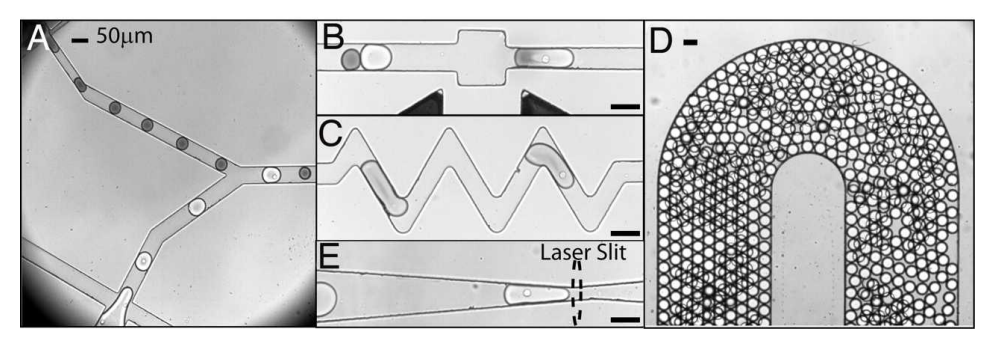
Brouzes E et al. PNAS 2009;106:14195-14200



Modules of the cell viability assay chip

- (A) Reinjection of incubated cells + encapsulation of viability test dye
- (B) Droplet fusion module (AC field)
- (C) Serpentine mixing module (cells with dyes)
- (D) Delay line for on-chip reaction (1.5 m!, 15 min)
- (E) Confinement for fluorescent detection





PDMS channels are 100 µm deep (D is 260 µm deep). Corresponding videos are in ESI of the article on the web-site.

Brouzes E et al. PNAS 2009;106:14195-14200

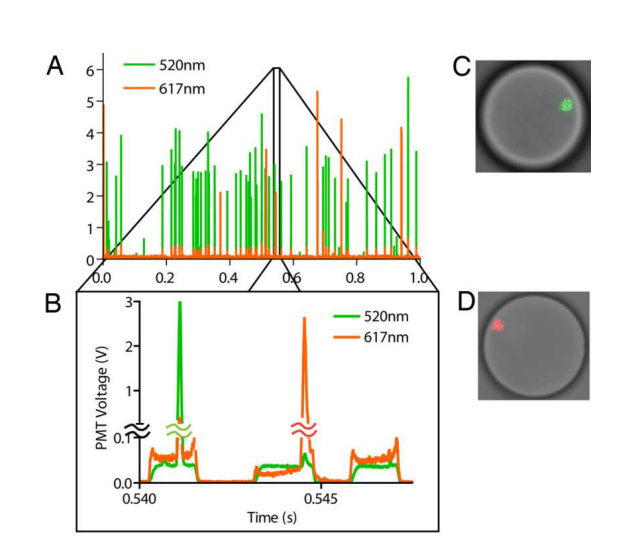
EPFL

Detection of live/dead cells

Interrogation of each droplet's fluorescence using laser line illumination and detection with photomultiplier tubes (PMTs) (≈100 drops/s).

Individual droplet signals decompose into a plateau (homogeneous droplet signal) overlaid by a narrow peak that corresponds to a cell.

Live/dead cells are stained with different fluorescent markers.



(A) Raw signal.

(B) 3 droplets, containing a live cell (λ =520 nm), a dead cell (λ =617 nm), and no cell, respectively.

(C and D) Images of droplets containing a live cell and a dead cell, respectively.

Brouzes E et al. PNAS 2009;106:14195-14200

Cytotoxicity drug screen

- (A) Optically encoded *mitomycin C* drug library with 8 different drug/dye concentrations.
- (B) The coding signal is collected at λ =710 nm, in addition to the stained cells (520 nm, 617 nm).
- (C) Dose-response curve of the assay (900 tests/data point).
- ⇒ Proof-of-concept of droplet microfluidics.
- ⇒ Throughput 100 Hz vs 1 compound test/s for conventional HTS systems.

Brouzes E et al. PNAS 2009;106:14195-14200

